Observational Study

Medicine®

OPEN

Intratumoral heterogeneity as measured using the tumor-stroma ratio and PET texture analyses in females with lung adenocarcinomas differs from that of males with lung adenocarcinomas or squamous cell carcinomas

Young Wha Koh, MD, PhD[a], Dakeun Lee, MD, PhD[a], Su Jin Lee, MD, PhD[b,*]

Abstract

We compared intratumoral stromal proportions and positron emission tomography (PET) textural features between females and males with lung adenocarcinoma (ADC) or squamous cell carcinoma (SCC).

We retrospectively evaluated 167 consecutive patients (male 122, female 45) who underwent pretreatment fluorodeoxyglucose PET/CT and surgical resection. The tumor-stroma ratios (TSRs) of primary tumors were estimated on hematoxylin-and-eosin-stained histological sections, and higher-order textural features were extracted on PET. We compared the histological and PET features between the sexes.

More females than males had ADC. Age and pathological tumor size did not significantly differ between females and males. Females with ADC had more stroma-rich tumors than males with ADC ($P = .016$) or SCC ($P = .047$). In addition, some PET textural features significantly differed between females with ADC and males with ADC and SCC; short run emphasis, long run emphasis, coarseness, strength, short-zone emphasis, zone percentage and high-intensity large-zone percentage were the commonly differed textural features. However, the TSRs and PET textural features did not significantly differ between males with ADC or SCC.

Intratumoral heterogeneity in females with lung ADC differs from that in males with lung ADC or SCC.

Abbreviations: ADC = adenocarcinoma, CT = computed tomography, FDG = fluorodeoxyglucose, MTV = metabolic tumor volume, NSCLC = nonsmall cell lung carcinoma, PET = positron emission tomography, SCC = squamous cell carcinoma, SUV = standardized uptake value, TLG = total lesion glycolysis, TSR = tumor-stroma ratio.

Keywords: adenocarcinoma of lung, female, positron emission tomography, texture analysis, tumor-stroma ratio

1. Introduction

Non-small cell carcinoma (NSCLC) is a heterogeneous disease. The biological features and treatment-related outcomes of lung adenocarcinoma (ADC) and squamous cell carcinoma (SCC) differ, although both are categorized as NSCLCs. In addition, the clinical characteristics of NSCLC differ between females and males in terms of median age at diagnosis, smoking history, predominant histological subtype, and treatment outcomes.[1,2] Although the reasons are complex, a large and growing body of literature has emphasized the important roles of estrogen and estrogen receptors in lung cancer development.[3–7] The effects of estrogen on the tumor microenvironment have been investigated in several types of cancer including lung cancer.[5,8,9]

Interplay among cancer, stromal, and immune cells and extracellular molecules of the tumor microenvironment are critical in cancer growth. Increasing evidence indicates that interactions between cancer cells and the neighboring stroma are important in cancer progression and metastasis.[10–12] Some investigations have focused on the intratumoral stromal proportion as a key regulator of cancer biology. The clinical significance of a high stromal proportion (the so-called high tumor-stroma ratio) in terms of cancer progression has been investigated in many types of cancers including those of the esophagus, stomach, breast, colon, and lung.[13–17]

F-18 fluorodeoxyglucose (FDG) positron emission tomography (PET)/computed tomography (CT) measures tumor glucose metabolism noninvasively, and is widely used to stage NSCLC. In addition, PET textural analyses have emerged as novel tools for assessing intratumoral heterogeneity. Texture analysis involves a series of calculations that evaluate the position and intensity of a digital image and extract information about the relationship between adjacent pixels.[18,19] Increasing evidence suggests that intratumoral heterogeneity can be characterized by PET textural

Editor: Neeraj Lalwani.

This work was supported by Basic Science Research Program through the National Research Foundation of Korea (NRF) funded by the Ministry of Science and ICT (NRF-2016R1C1B2011583).

The authors have no conflicts of interest to disclose.

[a] Department of Pathology, [b] Department of Nuclear Medicine, Ajou University School of Medicine, Suwon, Republic of Korea.

[*] Correspondence: Su Jin Lee, Department of Nuclear Medicine, Ajou University School of Medicine, 164, Worldcup-ro, Yeongtong-gu, Suwon 16499, Republic of Korea (e-mail: suesj202@ajou.ac.kr).

Medicine (2019) 98:11(e14876)

Received: 13 July 2018 / Received in final form: 24 October 2018 / Accepted: 21 February 2019

http://dx.doi.org/10.1097/MD.0000000000014876

analysis and that these features are related to clinical outcome such as treatment response or survival prediction in lung cancer.[20–23]

We previously reported that heterogeneity imaging parameters are significantly associated with the intratumoral stromal proportion in head and neck squamous cell carcinoma.[24] We hypothesized that heterogeneity imaging parameters might reflect the tumor microenvironment, and thus differ between sexes in NSCLCs. Therefore, we measured tumor-stroma ratios (TSRs) and PET textural features of primary NSCLCs, and evaluated the differences between females and males.

2. Materials and methods

2.1. Patients

We retrospectively reviewed the pretreatment FDG PET/CT scans of 275 consecutive NSCLC patients who underwent surgical treatment at a single institution (Ajou University Hospital, Suwon, Korea). Those with small malignant nodules (<1 cm in diameter) and histological cancer subtypes other than adenocarcinoma (ADC) or squamous cell carcinoma (SCC) were excluded. We ultimately evaluated 167 patients with lung ADC or SCC. Our ethics committee approved this retrospective study and waived the requirement for informed patient consent.

2.2. FDG PET/CT acquisition

FDG PET/CT was performed using the Discovery STE PET/CT scanner (GE Healthcare, Milwaukee, WI). All patients fasted for at least 6 hours before FDG PET/CT; their serum glucose levels at the time of FDG injection were <150 mg/dL. Unenhanced CT was performed 60 minutes after injection of 5 MBq/kg FDG, using a 16-slice helical CT scanner (120 keV; 30–100 mA in the AutomA mode; section width=3.75 mm). Emission PET data were acquired from the thigh to the head for 3.0 minutes per frame in the 3-dimensional mode. Attenuation-corrected PET images using CT data were reconstructed by an ordered-subset expectation maximization algorithm (20 subsets, 2 iterations).

2.3. PET texture analyses

The PET texture analysis method was previously described.[25] For tumor delineation, we used the gradient-based segmentation method (PET Edge) in MIM version 6.4 (MIM Software Inc., Cleveland, OH). Texture analysis for the quantification of intratumor heterogeneity on PET was performed using the Chang-Gung Image Texture Analysis toolbox (CGITA, https://code.google.com/archive/p/cgita), an open-source software package implemented in MATLAB (version 2012a; MathWorks Inc., Natick, MA).[26] Of the many textural matrices that can be derived using CGITA, 27 higher-order textural features were analyzed, because these features are commonly evaluated by medical imaging researchers.[19,25] Higher order textural features included gray level run length matrix, neighborhood gray level difference matrix, and gray level size zone matrix. After resampling with 64 discrete bins, we derived 27 higher order textural features. We also measured conventional PET parameters including the maximum standardized uptake value (SUVmax), metabolic tumor volume (MTV), and total lesion glycolysis (TLG) of the primary tumors.

2.4. Histopathology

Histological subclassification was performed by 2 pathologists (YWK and DL) based on the 2015 World Health Organization Classification of Lung Tumors.[27] To perform a differential diagnosis between ADC and SCC, we conducted immunohistochemical stainings for TTF-1, Napsin A and p40. TSRs were obtained by consensus. The stromal proportion was quantified as previously described.[16,24] In brief, the largest invasive tumor block was selected using the 1.25× objective. Subsequently, using the 10x objective, fields were only scored where both stroma and tumor were present, and the tumor cells were visible on all slides in the microscopic image field. Then the stromal proportion was estimated and scored in increments of 5 percentage points (e.g., 15%, 20%, and 25%). Representative photomicrographs are presented in Figure 1. All slides were reviewed in a blinded manner.

2.5. Statistical analyses

We expressed data as means ± SDs for continuous variables and as percentages for categorical variables. All analyses were conducted using SPSS for Windows software (ver 18.0; IBM Inc., New York, NY). Differences between the 2 groups were compared using the *t*-test for continuous variables and the chi-square test for dichotomous variables. *P* values <.05 were considered to indicate statistical significance.

3. Results

3.1. Patient characteristics

Of the 167 patients, 45 were females (26.9%) and 122 males (73.1%) of a mean age of 63.3 ± 9.2 years. The mean diameter of

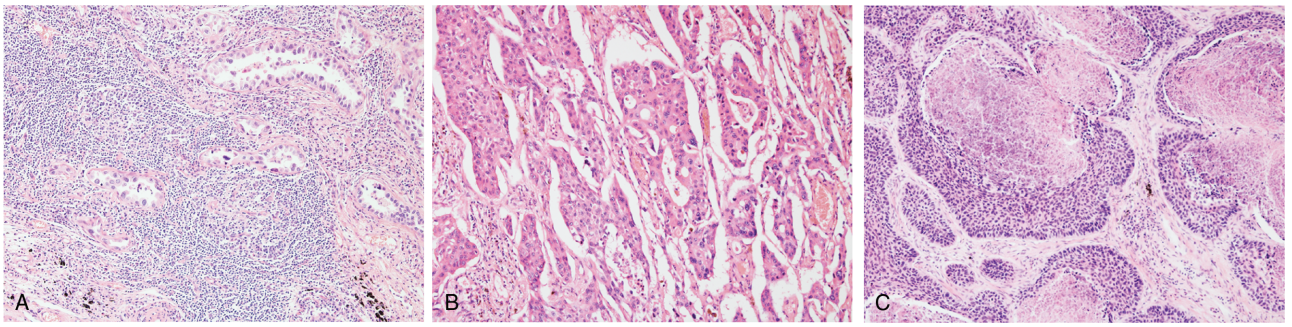

Figure 1. Representative photomicrographs of nonsmall cell carcinoma. (A) Female adenocarcinoma with a stromal proportion estimated as 60%. (B) Male adenocarcinoma with a stromal proportion estimated as 20%. (C) Male squamous cell carcinoma with a stromal proportion estimated as 20%.

Table 1

Clinical characteristics of 167 patients.

	Females (n = 45)	Males (n = 122)	*P* value
Age (mean ± sd)	61.2 ± 10.5	64.1 ± 8.5	.063
Smoking history	11 (24.4%)	106 (86.9%)	<.0001
Histology			
Adenocarcinoma	37 (82.2%)	58 (47.5%)	<.001
Squamous cell carcinoma	8 (17.8%)	64 (52.5%)	
Tumor size, cm	3.3 ± 1.3	3.6 ± 1.3	.180
Tumor stroma ratio, %	32.3 ± 13.2	29.2 ± 13.1	.175
Stroma-rich tumors	19 (42.2%)	30 (24.6%)	.026

resected primary tumors was 3.5 ± 1.3 cm (range, 1.2–7.0 cm). The clinical characteristics of females and males are summarized in Table 1. More males than females had smoking history. More females than males had ADC. Age, pathological tumor size, and TSR did not significantly differ between females and males. Stroma-rich and stroma-poor tumors were distinguished using the median TSR value (30). The proportion of stroma-rich tumors (TSR > 30) was significantly higher in females than in males (42.2 vs 24.6%, $P = .026$). We created 4 subgroups by sex and histology: females with ADC (F_{ADC}, n = 37), females with SCC (F_{SCC}, n = 8), males with ADC (M_{ADC}, n = 58), and males with SCC (M_{SCC}, n = 64). Figure 2 shows the differences in proportions of stroma-rich and stroma-poor tumors. We excluded the F_{SCC} subgroup from statistical analyses because of the small number of patients. The F_{ADC} subgroup had more stroma-rich tumors than the M_{ADC} subgroup (45.9 vs 22.4%, $P = .016$) and the M_{SCC} subgroup (45.9 vs 26.6%, $P = .047$); however, the M_{ADC} and M_{SCC} subgroups did not significantly differ ($P = .679$).

3.2. Differences in PET textural features according by sex and histology

The mean SUVmax, MTV, and TLG of females were 8.6 ± 4.8, 20.7 ± 30.5, and 107.1 ± 214.7, respectively; and 11.0 ± 6.6, 30.0 ± 38.4, and 181.9 ± 246.6, for males, respectively, who had a significantly higher SUVmax than females ($P = .033$). The MTV and TLG did not significantly differ between the sexes.

The higher order PET textural features of the 3 subgroups (F_{ADC}, M_{ADC}, and M_{SCC}) are summarized in Tables 2–4 (gray-level run length matrix, neighborhood gray-level difference matrix, and gray-level size zone matrix, respectively). Significant differences were evident between F_{ADC} and M_{ADC} and F_{ADC} and M_{SCC}, but not between M_{ADC} and M_{SCC}. The textural features that differed commonly were the short run emphasis, long run emphasis, coarseness, strength, short-zone emphasis, zone percentage and high-intensity large-zone percentage.

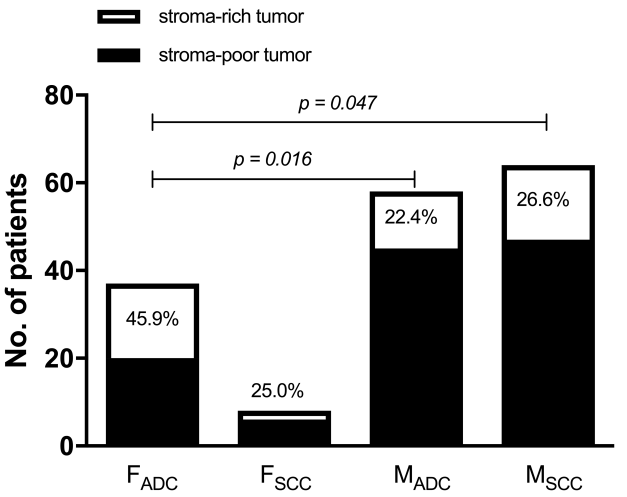

Figure 2. The difference of stroma-rich tumors among 4 subgroups. F_{ADC} = females with adenocarcinoma, F_{SCC} = females with squamous cell carcinoma, M_{ADC} = males with adenocarcinoma, M_{SCC} = males with squamous cell carcinoma.

4. Discussion

We found that intratumoral heterogeneity as measured using TSR and PET textural analyses significantly differed between females and males. Histopatholgically, F_{ADC} had more tumors with high proportions of stroma. Interestingly, we found no significant difference between M_{ADC} and M_{SCC}. The PET data yielded similar results: some textural features significantly differed between F_{ADC} and M_{ADC} and F_{ADC} and M_{SCC}, but not between M_{ADC} and M_{SCC}.

Intratumoral heterogeneity measured by imaging modalities such as PET or CT may be associated with differences in regional tumor cellularity, proliferation, hypoxia, necrosis, and angiogenesis.[28,29] These heterogeneous biological characteristics may be related with the tumor–stroma interaction. Cancer-associated fibroblasts (CAFs), the main cellular components of the stroma, may play a critical role in the tumor–stroma interaction. The accumulation of fibrotic extracellular matrix is induced by CAFs and the structure of the extracellular matrix can be further

Table 2

Comparison of gray-level run length matrix.

	F_{ADC}	M_{ADC}	*P* value (vs F_{ADC})	M_{SCC}	*P* value (vs F_{ADC})
Short run emphasis	0.85 ± 0.10	0.78 ± 0.12	.005	0.08 ± 0.13	.003
Long run emphasis	1.61 ± 0.42	1.92 ± 0.56	.004	1.96 ± 0.61	.003
Intensity variability	9.32 ± 16.03	27.72 ± 99.09	.266	24.22 ± 37.33	.023
Run-length variability	186.30 ± 318.20	344.76 ± 608.00	.147	361.19 ± 425.09	.032
Run percentage	0.61 ± 0.10	0.64 ± 0.14	.345	0.64 ± 0.14	.330
Low-intensity run emphasis	0.02 ± 0.02	0.02 ± 0.01	.060	0.03 ± 0.03	.877
High-intensity run emphasis	897.07 ± 190.58	915.13 ± 264.87	.720	854.45 ± 275.34	.407
Low-intensity short-run emphasis	0.02 ± 0.02	0.02 ± 0.01	.027	0.02 ± 0.02	.747
High-intensity short-run emphasis	761.70 ± 205.72	719.35 ± 227.66	.361	670.07 ± 238.58	.056
Low-intensity long-run emphasis	0.04 ± 0.03	0.03 ± 0.04	.622	0.05 ± 0.10	.464
High-intensity long-run emphasis	1450.73 ± 531.78	1735.21 ± 694.89	.036	1615.62 ± 724.05	.230

Table 3

Comparison of neighborhood gray-level difference matrix.

	F_{ADC}	M_{ADC}	*P* value (vs F_{ADC})	M_{SCC}	*P* value (vs F_{ADC})
Coarseness	0.04 ± 0.02	0.03 ± 0.02	.017	0.03 ± 0.02	.002
Contrast	0.14 ± 0.27	0.04 ± 0.11	.020	0.59 ± 3.21	.395
Busyness	0.09 ± 0.09	0.15 ± 0.16	.078	0.16 ± 0.16	.018
Complexity	102.64 ± 79.60	66.85 ± 70.65	.024	75.61 ± 106.72	.184
Strength	48.32 ± 19.49	38.92 ± 19.08	.022	37.04 ± 20.20	.007

Table 4

Comparison of gray-level size zone matrix.

	F_{ADC}	M_{ADC}	*P* value (vs F_{ADC})	M_{SCC}	*P* value (vs F_{ADC})
Short-zone emphasis	0.86 ± 0.07	0.82 ± 0.06	.007	0.82 ± 0.07	.012
Large-zone emphasis	2.04 ± 0.94	5.31 ± 20.70	.341	4.05 ± 7.28	.099
Intensity variability	4.40 ± 5.25	6.59 ± 6.28	.081	7.44 ± 7.03	.024
Size-zone variability	106.82 ± 132.27	158.18 ± 142.50	.082	175.65 ± 158.19	.028
Zone percentage	0.46 ± 0.12	0.41 ± 0.10	.017	0.40 ± 0.13	.018
Low-intensity zone percentage	0.03 ± 0.02	0.02 ± 0.01	.039	0.03 ± 0.02	.565
High-intensity zone percentage	870.33 ± 176.65	883.81 ± 181.31	.722	838.46 ± 188.32	.404
Low-intensity short-zone percentage	0.02 ± 0.02	0.02 ± 0.01	.042	0.02 ± 0.02	.490
High-intensity short-zone percentage	756.83 ± 199.37	726.56 ± 168.32	.429	691.32 ± 182.21	.096
Low-intensity large-zone percentage	0.05 ± 0.04	0.20 ± 1.17	.440	0.15 ± 0.58	.314
High-intensity large-zone percentage	1802.47 ± 1151.02	2348.76 ± 1341.05	.044	2301.73 ± 1200.89	.044

stimulated and altered by proteases, which degrade the stroma. Together, these cause the destruction of epithelial tissue and remodeling of the extracellular matrix, thereby promoting the invasion of tumor cells. CAFs also secrete growth factors, inflammatory factors, and angiogenic factors, all of which contribute to intratumoral heterogeneity.[30,31] It has been suggested that increased image heterogeneity is associated with more aggressive tumor behavior, poorer response to treatment and worse prognosis.[19] Because clinical characteristics between sexes in NSCLC are apparent, we hypothesized that the intratumoral heterogeneity between females and males is different. Therefore, we chose TSR as a possible histopathologic feature to compare PET textural features between females and males although little is known what the biological correlates of textural features are.

NSCLC-specific research has demonstrated that stroma in NSCLC is associated with tumor invasiveness, metastasis and poor prognosis. Nakamura et al[32] showed that the expression of carbonic anhydrase IX by CAFs contributed to an increase in aggressive behavior in lung ADC with hypoxic regions. Takahashi et al[33] reported that SCC with a fibrous stroma displayed higher invasive phenotype and were associated with a significantly poor prognosis.

Recently, texture analysis has been identified as a tool for "radiomics" on medical images. Recent investigations using texture analyses by FDG PET and chest CT showed that some textural features of ADC and SCC differed, thus radiomic signature can be used to distinguish lung ADC from SCC.[18,34] Here, we found differences in PET textural features by sex and histological subtype, consistent with the different proportions of high-stroma tumors among the subgroups. Thus, tumor biology may differ by sex in addition to histological subtype; females with lung ADC differed from that of males with lung ADC or SCC. This result suggests that lung ADC and SCC may require a sex-specific PET radiomic approach.

Our study had several limitations. Patient numbers were relatively small and all had relatively early stage lung cancers; we only included surgically treated patients. We excluded females with SCC from statistical analyses because of the small number of patients; the female SCC incidence is rather low. Further studies with larger cohorts are required.

5. Conclusion

Intratumoral heterogeneity measured using TSR and PET textural analyses in females with lung ADC differed from that of males with lung ADC or SCC.

Author contributions

Conceptualization: Young Wha Koh, Dakeun Lee.
Data curation: Dakeun Lee.
Formal analysis: Young Wha Koh, Dakeun Lee, Su Jin Lee.
Funding acquisition: Su Jin Lee.
Methodology: Young Wha Koh, Dakeun Lee, Su Jin Lee.
Supervision: Su Jin Lee.
Visualization: Young Wha Koh, Su Jin Lee.
Writing – original draft: Young Wha Koh, Su Jin Lee.
Writing – review & editing: Dakeun Lee, Su Jin Lee.
Su Jin Lee orcid: 0000-0002-2096-6115.

References

[1] De Matteis S, Consonni D, Pesatori AC, et al. Are women who smoke at higher risk for lung cancer than men who smoke? Am J Epidemiol 2013;177:601–12.
[2] Donington JS, Colson YL. Sex and gender differences in non-small cell lung cancer. Semin Thorac Cardiovasc Surg 2011;23:137–45.
[3] Rodriguez-Lara V, Hernandez-Martinez JM, Arrieta O. Influence of estrogen in non-small cell lung cancer and its clinical implications. J Thorac Dis 2018;10:482–97.

[4] Hsu LH, Liu KJ, Tsai MF, et al. Estrogen adversely affects the prognosis of patients with lung adenocarcinoma. Cancer Sci 2015;106:51–9.
[5] Siegfried JM, Stabile LP. Estrongenic steroid hormones in lung cancer. Semin Oncol 2014;41:5–16.
[6] Katcoff H, Wenzlaff AS, Schwartz AG. Survival in women with NSCLC: the role of reproductive history and hormone use. J Thorac Oncol 2014;9:355–61.
[7] Stabile LP, Dacic S, Land SR, et al. Combined analysis of estrogen receptor beta-1 and progesterone receptor expression identifies lung cancer patients with poor outcome. Clin Cancer Res 2011;17: 154–64.
[8] Daniels G, Gellert LL, Melamed J, et al. Decreased expression of stromal estrogen receptor alpha and beta in prostate cancer. Am J Transl Res 2014;6:140–6.
[9] Pequeux C, Raymond-Letron I, Blacher S, et al. Stromal estrogen receptor-alpha promotes tumor growth by normalizing an increased angiogenesis. Cancer Res 2012;72:3010–9.
[10] Quail DF, Joyce JA. Microenvironmental regulation of tumor progression and metastasis. Nat Med 2013;19:1423–37.
[11] Junttila MR, de Sauvage FJ. Influence of tumour micro-environment heterogeneity on therapeutic response. Nature 2013;501:346–54.
[12] Joyce JA, Pollard JW. Microenvironmental regulation of metastasis. Nat Rev Cancer 2009;9:239–52.
[13] Xi KX, Wen YS, Zhu CM, et al. Tumor-stroma ratio (TSR) in non-small cell lung cancer (NSCLC) patients after lung resection is a prognostic factor for survival. J Thorac Dis 2017;9:4017–26.
[14] Wang K, Ma W, Wang J, et al. Tumor-stroma ratio is an independent predictor for survival in esophageal squamous cell carcinoma. J Thorac Oncol 2012;7:1457–61.
[15] de Kruijf EM, van Nes JG, van de Velde CJ, et al. Tumor-stroma ratio in the primary tumor is a prognostic factor in early breast cancer patients, especially in triple-negative carcinoma patients. Breast Cancer Res Treat 2011;125:687–96.
[16] Mesker WE, Junggeburt JM, Szuhai K, et al. The carcinoma-stromal ratio of colon carcinoma is an independent factor for survival compared to lymph node status and tumor stage. Cell Oncol 2007;29:387–98.
[17] Lee D, Ham IH, Son SY, et al. Intratumor stromal proportion predicts aggressive phenotype of gastric signet ring cell carcinomas. Gastric Cancer 2017;20:591–601.
[18] Ha S, Choi H, Cheon GJ, et al. Autoclustering of non-small cell lung carcinoma subtypes on (18)F-FDG PET using texture analysis: a preliminary result. Nucl Med Mol Imaging 2014;48:278–86.
[19] Chicklore S, Goh V, Siddique M, et al. Quantifying tumour heterogeneity in 18F-FDG PET/CT imaging by texture analysis. Eur J Nucl Med Mol Imaging 2013;40:133–40.
[20] Koh YW, Park SY, Hyun SH, et al. Associations between PET textural features and GLUT1 expression, and the prognostic significance of textural features in lung adenocarcinoma. Anticancer Res 2018;38: 1067–71.
[21] Kirienko M, Cozzi L, Antunovic L, et al. Prediction of disease-free survival by the PET/CT radiomic signature in non-small cell lung cancer patients undergoing surgery. Eur J Nucl Med Mol Imaging 2018;45: 207–17.
[22] Lovinfosse P, Janvary ZL, Coucke P, et al. FDG PET/CT texture analysis for predicting the outcome of lung cancer treated by stereotactic body radiation therapy. Eur J Nucl Med Mol Imaging 2016;43:1453–60.
[23] Cook GJ, O'Brien ME, Siddique M, et al. Non-small cell lung cancer treated with erlotinib: heterogeneity of (18)F-FDG uptake at PET-association with treatment response and prognosis. Radiology 2015;276: 883–93.
[24] Choi JW, Lee D, Hyun SH, et al. Intratumoural heterogeneity measured using FDG PET and MRI is associated with tumour-stroma ratio and clinical outcome in head and neck squamous cell carcinoma. Clin Radiol 2017;72:482–9.
[25] Hyun SH, Kim HS, Choi SH, et al. Intratumoral heterogeneity of (18)F-FDG uptake predicts survival in patients with pancreatic ductal adenocarcinoma. Eur J Nucl Med Mol Imaging 2016;43:1461–8.
[26] Fang YH, Lin CY, Shih MJ, et al. Development and evaluation of an open-source software package "CGITA" for quantifying tumor heterogeneity with molecular images. Biomed Res Int 2014;2014: 248505.
[27] Travis WD, Brambilla E, Nicholson AG, et al. The 2015 World Health Organization Classification of Lung Tumors: impact of genetic, clinical and radiologic advances since the 2004 classification. J Thorac Oncol 2015;10:1243–60.
[28] Ganeshan B, Goh V, Mandeville HC, et al. Non-small cell lung cancer: histopathologic correlates for texture parameters at CT. Radiology 2013;266:326–36.
[29] Tixier F, Le Rest CC, Hatt M, et al. Intratumor heterogeneity characterized by textural features on baseline 18F-FDG PET images predicts response to concomitant radiochemotherapy in esophageal cancer. J Nucl Med 2011;52:369–78.
[30] Egeblad M, Werb Z. New functions for the matrix metalloproteinases in cancer progression. Nat Rev Cancer 2002;2:161–74.
[31] Kalluri R, Zeisberg M. Fibroblasts in cancer. Nat Rev Cancer 2006;6:392–401.
[32] Nakamura H, Ichikawa T, Nakasone S, et al. Abundant tumor promoting stromal cells in lung adenocarcinoma with hypoxic regions. Lung Cancer 2018;115:56–63.
[33] Takahashi Y, Ishii G, Taira T, et al. Fibrous stroma is associated with poorer prognosis in lung squamous cell carcinoma patients. J Thorac Oncol 2011;6:1460–7.
[34] Zhu X, Dong D, Chen Z, et al. Radiomic signature as a diagnostic factor for histologic subtype classification of non-small cell lung cancer. Eur Radiol 2018;28:2772–8.